ASYMMETRIC SPEED-DEPENDENT SPECTRAL LINE SHAPES IN CADMIUM-FOREIGN-GAS SYSTEMS*

A. Bielski, R. Ciuryło, J. Domysławska, D. Lisak, J. Szudy and R.S. Trawiński

Institute of Physics, Nicholas Copernicus University
Grudziądzka 5, 87-100 Toruń, Poland

(Received June 3, 2002)

Results of a series of experiments on collisional and speed-dependent effects caused by various foreign gases on the 326.1 nm Cd intercombination line are discussed in detail. Using a laser-induced fluorescence method precise measurements of pressure-broadened profiles of this line perturbed by all rare gases and some molecular gases (H_2, D_2, N_2 and CH_4) were performed in our laboratory at pressures up to 400 Torr. The line shapes were analyzed in terms of a Speed-Dependent Asymmetric Voigt Profile (SDAVP) and the role of the correlation between pressure broadening rate and emitter velocity as well as of the finite duration of collisions were thoroughly investigated. These effects were found to be particularly important in the cases of perturbation by heavy, *i.e.* high-polarizability rare-gas atoms (Ar, Kr, Xe). Pressure-broadening and shift rates and the collision-time asymmetry factors as well as effective cross sections for the broadening and shifting of the 326.1 nm Cd line were determined and compared with those calculated on the basis of the van der Waals, Morse and Czuchaj–Stoll potentials.

PACS numbers: 32.70.–n, 33.70.–w, 34.20.–b

1. Introduction

During the past two decades several detailed studies of the profiles of pressure-broadened atomic and molecular spectral lines have been undertaken using laser excitation techniques which allowed precise measurements of fine features of the intensity distribution in the core and near-wing regions [1–14]. For many years the theoretical interpretation of experimental line profiles at low pressures was performed using an impact theory in which the

* Presented at the Photons, Atoms and All That, PAAT 2002 Conference, Cracow Poland, May 31–June 1, 2002.

radiation emitted during a collision time is neglected. The impact theory predicts then for the intensity distribution purely Lorentzian form with the width (FWHM) γ and the shift Δ of the maximum of the line linearly dependent on the density number N of perturbers. Traditionally, the Doppler broadening caused by thermal motion of emitting atoms with Maxwellian distribution of velocities was treated as the effect statistically independent of the pressure broadening and the resulting line shape was presented as a convolution of the Lorentzian and Gaussian profiles known as the Voigt Profile (VP). However, the use of high-resolution laser spectroscopy technique has enabled to reveal departures of the measured spectral line shapes from the VP. These departures were identified as arising from two distinct sources: (1) *the breakdown of the impact theory* and necessity of taking into account effects due to the *finite duration* of collisions, and (2) *the correlation between pressure and velocity* contributions to the line shape.

The first-order correction to the Lorentzian profile coming from the finite duration of collisions was shown [2, 7–9, 17–21] to have a dispersion shape proportional to the collision duration time. The resulting line shape being the sum of the Lorentzian and dispersion profiles becomes then asymmetric with respect to the position of the line peak. This type of asymmetry is usually referred to as the *collision-time asymmetry* in order to distinguish it from that caused by the *correlation between the collisional broadening and thermal motion* of the emitter. Collision correlation effects have been theoretically analyzed first by Rautian and Sobelman [22], Berman [23] and Ward *et al.* [24]. A direct manifestation of these effects appears when the experimental profile is fitted to the VP. If these effects are present then, as was shown by Ward *et al.* [24], the width γ_{D} of the Gaussian component of the VP (usually identified with the Doppler width of the line) which results from such a fit should decrease with increasing perturbing gas pressure. The collision correlation effects become increasingly apparent with increasing values of $\alpha = m_{\mathrm{p}}/m_{\mathrm{e}}$, the ratio of the mass of perturber to emitter. This means that for heavier perturbers collision correlation effects cannot be ignored and the complete analysis of the pressure-broadened spectral line shape should be performed in such a way that both the effects due to the finite duration of collisions and the collision correlation are taken into account. The simplest way to analyze the modification of the collisional component of the resultant line shape due to this correlation is to express the parameters describing the pressure-broadened profile as a function of the velocity of emitter and then to perform the convolution of this profile with the Maxwellian distribution. Following Berman [23] and Harris *et al.* [7] the convolution of the Lorentzian profile characterized by speed-dependent Lorentzian width $\gamma = \gamma(v)$ and shift $\Delta = \Delta(v)$ with the Gaussian distribution will be referred to as the Speed-Dependent Voigt Profile (SDVP). The line shapes resulting from the convolution of the Gaussian distribution with the sum of the Lorentzian profile and the first-order dispersion correction to it will be referred to as the speed-dependent asymmetric Voigt profile.

The first experimental observations of the collision-time asymmetry were reported in 1980 by Kielkopf and Allard [1] and Walkup *et al.* [2] and later by Raymond *et al.* [3] and other workers [4–6]. No effort was made, however, in these studies to include the influence of speed-dependent effects on the observed profiles. The first experiments in which both the finite duration of collisions and the speed-dependent correlation between the pressure and Doppler broadening were taken into account were performed by Lewis and his co-workers [7–9] for the calcium 422.7 nm resonance line perturbed by rare gases. Until the end of 1990's calcium remained the only element for which the complete analysis of the line shape was made. Because of the lack of experimental data for other elements we have undertaken in our laboratory systematic studies of the pressure and Doppler broadening of the 326.1 nm intercombination line of cadmium interacting with various foreign gases [11–14].

The choice of Cd as an active atom was motivated by recent theoretical work by Czuchaj and Stoll [15] who carried out *ab initio* calculations of potential energy curves for Cd, rare gas systems as well as recent experiments on Cd, rare gas excimers created in supersonic expansion done by Koperski *et al.* [16]. As was already indicated by the Lewis group [7–9] because of the similarity between contributions from collision duration and speed-dependent correlation effects an extreme care is required in any experimental study dealing with quantitative estimation of contributions from these two sources. Our measurements were performed using a method of Laser-Induced Fluorescence (LIF). The good signal to noise ratio and negligible instrumental function enabled us to fit our experimental line shapes to the improved theoretical profiles such as SDVP or SDAVP in considerable detail and identify departures from the ordinary VP which can be ascribed to the finite collision duration and (or) speed-dependent effects. In the present paper the experimental results are discussed and compared with theoretical expectations.

2. Experimental

Here we shall give only a brief description of the experimental procedure based on the LIF method; details may be found elsewhere [11–14]. A Coherent CR 899-21 ring dye laser equipped with intracavity frequency doubler CR 8500 pumped by INNOVA-400 argon-ion laser provided single mode UV output which was continuously scanned in frequency up to 60 GHz across the region of the 326.1 nm Cd intercombination line. The instrumental width of the laser is about 1 MHz or $3.3 \times 10^{-5}\,\mathrm{cm}^{-1}$. Laser radiation was absorbed by cadmium vapor in the presence of perturbing gas and Cd-atoms were excited to the $5\ {}^3\mathrm{P}_1$ state. In order to avoid problems with hyperfine and isotope structure of the line the ^{114}Cd isotope was used. The fluorescence cells containing this isotope were filled with foreign gas and cut-off from the vacuum system and then mounted in an oven at temperature of 450 K. By measuring the total intensity of the light emitted from the $5^3\mathrm{P}_1$ state as a function of the detuning of the ring laser the intensity distribution within the line was obtained.

3. The collision time asymmetry

As was established first by Anderson and Talman [17] and later discussed by several workers [2, 7–9, 19–21] the modification of the line profile due to the finite duration of collision can be described by the addition of the dispersion component to the ordinary Lorentzian shape. The resulting profile becomes then [19–21]

$$I(\omega) = \frac{1}{2\pi}\frac{\Gamma(\omega)}{(\omega-\omega_0-\Delta)^2+\left(\frac{\gamma}{2}\right)^2}\,, \tag{1}$$

where ω_0 is the unperturbed frequency, γ and Δ are the full Lorentzian width (FWHM) and shift of the line. Here $\Gamma(\omega)$ is the frequency-dependent broadening rate which in the first-order approximation can be written as [7–9, 19]

$$\Gamma(\omega) = \gamma + \chi(\omega-\omega_0-\Delta)\,, \tag{2}$$

where χ denotes the collision-time asymmetry factor. Starting from the Anderson–Baranger line broadening theory [17,18] Ciuryło *et al.* [25] have been able to express χ in terms of the elements of time-evolution operators or, in classical limit, in terms of phase-shift functions which are determined by $\Delta V(r) = V_{\mathrm{u}}(r) - V_{\mathrm{l}}(r)$, the difference of adiabatic potentials in the upper (u) and lower (l) state of the emitting atom, respectively, written as functions of the distance $r = r(t)$ between emitter and the perturber at time t. For the van der Waals potential

$$V(r) = -\hbar\,\Delta C_6 r^{-6}\,, \tag{3}$$

the classical impact-parameter calculations have been shown [19] to give

$$\gamma = 8.08278\,NvR_0^2\,, \tag{4}$$

$$\Delta = 2.93624\,NvR_0^2\,, \tag{5}$$

and

$$\chi = 5.43542\, N R_0^3\,, \tag{6}$$

where

$$R_0 = \left(\frac{\Delta C_6}{v}\right)^{1/5} \tag{7}$$

is the Weisskopf radius. Let us note that Eq. (6) can be re-written in the form

$$\chi = 0.67247\, \gamma \tau_{\rm d}\,, \tag{8}$$

where

$$\tau_{\rm d} = \frac{R_0}{v} = |\Delta C_6|^{1/5} v^{-6/5} \tag{9}$$

is the collision duration time.

In the traditional line shape analysis the Lorentzian width and shift are often discussed in terms of the cross sections $\sigma_{\rm b}$ and $\sigma_{\rm s}$ for the collision broadening and shifting, respectively, according to definitions: $\gamma = N v \sigma_{\rm b}$ and $\Delta = \pm N v \sigma_{\rm s}$, where v is the relative velocity. In the Coulomb approximation [26] $\Delta C_6 = A\xi$, where ξ is the polarizability of the perturber and $A = e^2[\langle r^2\rangle_{\rm u} - \langle r^2\rangle_{\rm l}]$. Here e is the elementary charge and $\langle r^2\rangle_{\rm u}$ (or $\langle r^2\rangle_{\rm l}$) denotes the expectation value of r^2 for the upper (or lower) state of the emitter. Using Eqs. (2)–(3) we obtain for the broadening and shifting cross sections

$$\sigma_{\rm b} = 8.08278\, A^{2/5} \left(\frac{\xi}{v}\right)^{2/5} \tag{10}$$

and

$$\sigma_{\rm s} = 2.93624\, A^{2/5} \left(\frac{\xi}{v}\right)^{2/5} . \tag{11}$$

We should emphasize, however, that the variations of cross sections with relative velocity depends on interatomic interactions so that, in general case, the broadening and shifting cross sections should be averaged over Maxwellian distribution.

4. Speed-dependent effects

In order to include the correlation between thermal motion of emitters and their collisions with perturbers, the line shape given by Eq. (1) must be averaged over the emitter velocities. Following Harris *et al.* [7–9] and Ciuryło [27, 11] the resulting line shape, called the speed-dependent asymmetric Voigt profile, can be written in the form

$$I(\omega) = \frac{4\sqrt{\ln 2}}{\pi^{3/2}\gamma_{\mathrm{D}}} \times \int\limits_{-\infty}^{\infty} dx \mathrm{e}^{-x^2} x \left\{ \arctan[A(x,\omega)] + \tfrac{1}{2}\langle\chi\rangle B_{\mathrm{A}}(x,\alpha) \ln[1+A^2(x,\omega)] \right\}, \quad (12)$$

where x is dimensionless emitter speed in units of the most probable emitter speed $u = (2kT/m_{\mathrm{e}})^{1/2}$, with m_{e} being the mass of the emitter, and

$$A(x,\omega) = \frac{\omega - \omega_0 - \langle\Delta\rangle B_{\mathrm{S}}(x,\alpha) + x\gamma_{\mathrm{D}}/(2\sqrt{\ln 2})}{\langle\gamma\rangle B_{\mathrm{W}}(x,\alpha)/2}. \quad (13)$$

Here $B_{\mathrm{W}}(x,\alpha) = \gamma(x,\alpha)/\langle\gamma\rangle$, $B_{\mathrm{S}}(x,\alpha) = \Delta(x,\alpha)/\langle\Delta\rangle$ and $B_{\mathrm{A}}(x,\alpha) = \chi(x,\alpha)/\langle\chi\rangle$ denote the reduced broadening, shift and asymmetry parameters, where $\langle\gamma\rangle$, $\langle\Delta\rangle$ and $\langle\chi\rangle$ are broadening, shift and asymmetry parameters averaged over the Maxwellian distribution of emitter velocities. In Eq. (12) $\gamma_{\mathrm{D}} = 2\sqrt{\ln 2}\,\omega_0 u/c$ is the Doppler width for the cell temperature T. The calculation of the above reduced parameters requires the knowledge of the difference $\Delta V(r)$ of interaction potentials. For the van der Waals potentials they can be expressed as [24]

$$B_{\mathrm{W}}(x,\alpha) = B_{\mathrm{S}}(x,\alpha) = (1+\alpha)^{-3/10} M\left(-\frac{3}{10}, \frac{3}{2}, -\alpha x^2\right), \quad (14)$$

and [11,14]

$$B_{\mathrm{A}}(x,\alpha) = (1+\alpha)^{3/10} M\left(\frac{3}{10}, \frac{3}{2}, -\alpha x^2\right), \quad (15)$$

where $M(a,b,c)$ is the confluent hyper-geometric function.

Using Eqs. (12), (13) the reduced broadening $B_{\mathrm{W}}(x,\alpha)$ and asymmetry $B_{\mathrm{A}(}x,\alpha)$ parameters were evaluated for the specific case of a van der Waals potential (vdW). Figs. 1 and 2 show plots of these parameters on the reduced speed x for various examples of α. It is seen that the correlation between pressure and Doppler broadening is considerable even for $\alpha \approx 0.5$. The role of this correlation strongly increases with the increase of α and for the value $\alpha = 22$ corresponding to the case of lithium perturbed by Xe studied by McCartan and Lwin [31] the correlation strength quickly approaches the asymptotic behavior $B_{\mathrm{W}}(x,\alpha) \propto v^{0.6}$ for $\alpha \to \infty$. It should be noted that for $\alpha \to 0$ all reduced quantities are equal to one ($B_{\mathrm{W}}(x,\alpha) = B_{\mathrm{S}}(x,\alpha) = B_{\mathrm{A}}(x,\alpha) = 1$) and this means that for light emitters and heavy perturbers speed-dependent effects can be completely ignored. Eq. (10) becomes then identical with the asymmetric Voigt profile (AVP) which can be identified with the ordinary VP for $\langle\chi\rangle = 0$, *i.e.* when the collision time is neglected.

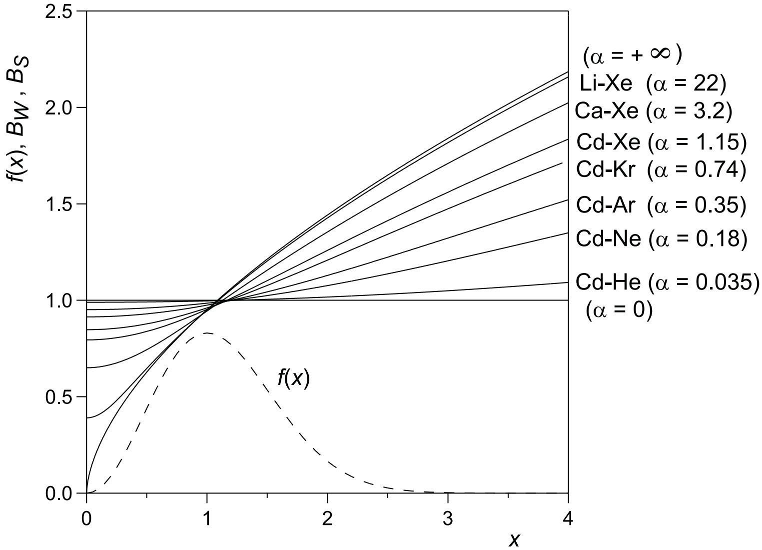

Fig. 1. Dependence of reduced broadening B_{W} and shift B_{S} parameters on reduced speed x for various perturber to emitter mass ratio α calculated for van der Waals potential ($f(x)$ Maxwellian distribution).

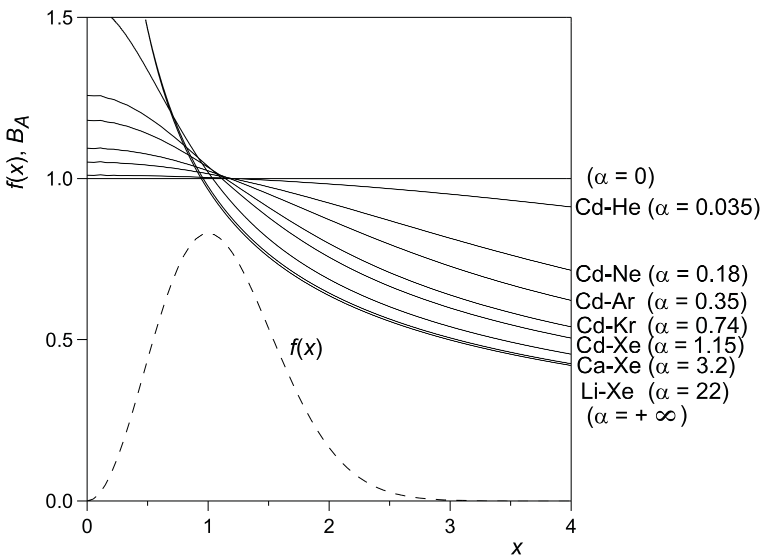

Fig. 2. Dependence of reduced asymmetry parameter B_{A} on reduced speed x for various perturber to emitter mass ratio α calculated for van der Waals potential ($f(x)$ Maxwellian distribution).

5. Results and discussion

5.1. Doppler collision correlation

Using the LIF technique we have measured the profiles of the 326.1 nm ^{114}Cd line perturbed by all rare gases at a range of pressures up to 400 Torr. For these perturbers the mass ratio α is equal to 0.035 for He, 0.18 for Ne, 0.35 for Ar, 0.74 for Kr and 1.15 for Xe. We have also measured profiles of this line perturbed by molecular gases such as H_2 ($\alpha = 0.0175$), D_2 ($\alpha = 0.0351$), and recently by N_2 ($\alpha = 0.2456$) and CH_4 ($\alpha = 0.1404$).

In order to examine the role of the Doppler collision correlation and the finite duration of collision in the formation of the spectral line shape we fitted our experimental profiles to four theoretical line-shape expressions discussed in preceding section: (1) ordinary Voigt profile (VP), (2) speed-dependent Voigt profile (SDVP), (3) asymmetric Voigt profile (AVP), and (4) speed-dependent asymmetric Voigt profile (SDAVP). The best-fit procedure was performed using a least-squares algorithm for nonlinear parameters due to Marquardt [28]. Our numerical fits to the VP and SDVP allowed three parameters to vary: the Doppler width γ_{D}, averaged Lorentzian width $\langle\gamma\rangle$ and the averaged shift $\langle\varDelta\rangle$. When fitting our experimental data to the AVP and SDAVP forms, four parameters were allowed to vary: γ_{D}, $\langle\gamma\rangle$, $\langle\varDelta\rangle$ and the collision-time asymmetry factor $\langle\chi\rangle$.

In the evaluation of the line shapes in terms of SDAVP we encountered serious difficulties due to the lack of accurate theoretical interaction potentials. For the Cd-rare-gas-atom systems the only theoretical potentials are those calculated by Czuchaj and Stoll (C–S) [15]. On the other hand, the long range attractive interactions can be described by the van der Waals (vdW) potentials. In our analysis both the C–S and vdW potentials were used to determine the speed-dependent reduced quantities $B_{\mathrm{W}}(x,\alpha)$, $B_{\mathrm{S}}(x,\alpha)$ and $B_{\mathrm{A}}(x,\alpha)$.

Following a procedure described by Harris *et al.* [7] a direct evidence of speed-dependent correlation effects can be obtained by analyzing the experimental line shape as if it were an AVP. Their existence appears then in the form of the narrowing of the Doppler component of this profile with the increase of the perturbing gas pressure at fixed cell temperature. Such a behavior which strongly depends on the perturber-to-emitter mass ratio α was observed in our experiments for Cd–Kr and Cd–Xe systems and is shown in Fig. 3, where the Doppler widths γ_{D} of the 326.1 nm Cd line determined from the fits of measured profiles to the AVP and SDAVP forms are plotted against the pressure of Xe (Fig. 3(a)) and Kr (Fig. 3(b)), Ar (Fig. 3(c)) and Ne (Fig. 3(d)). As it is seen both for Xe and Kr the Doppler width determined by fitting data to AVP by a least-squares minimalisation method decreases markedly with increasing pressure. On the other hand,

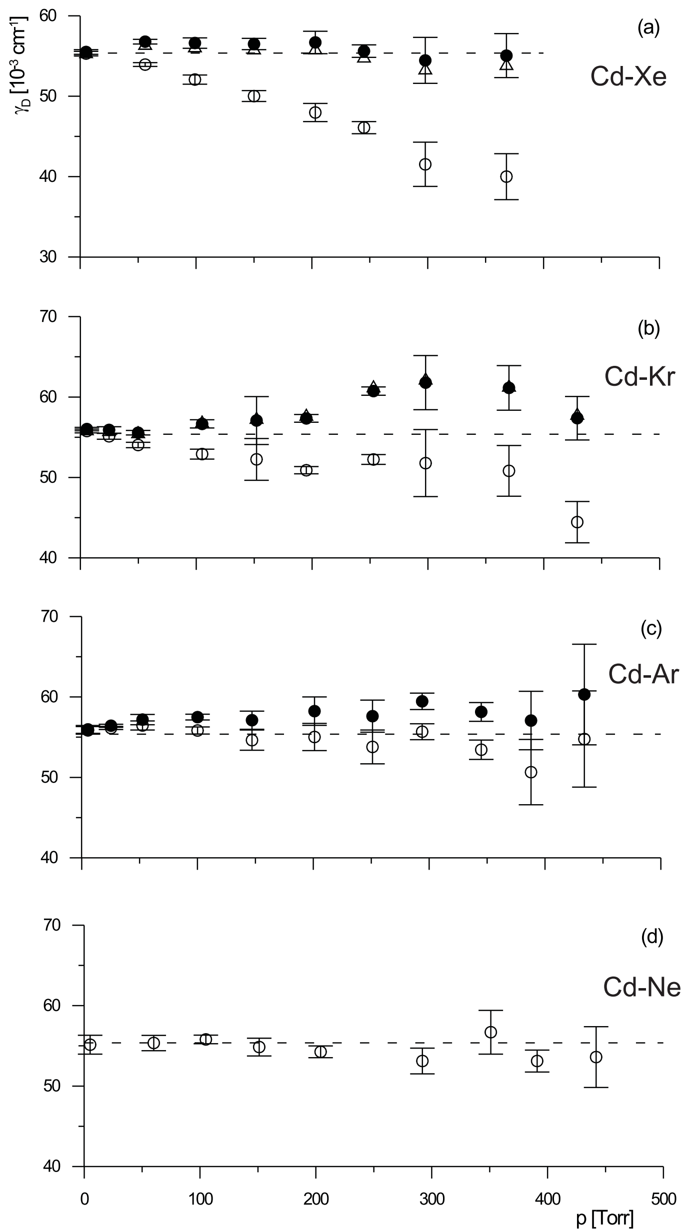

Fig. 3. Doppler width γ_D of fitted AVP (open circles ∘ (a)–(d)) and SDAVP (dots • using Czuchaj–Stoll potential [15] (a)–(c), triangles △ using the van der Waals potential (a)–(b)) to the measured 326.1 nm Cd line profile perturbed by Xe (a), Kr (b), Ar (c) and Ne (d).

the Doppler width determined by fitting data to the SDAVP is roughly constant for all krypton or xenon pressures, although the mean value of γ_D is slightly higher than the value $\gamma_D = 0.055$ cm^{-1} expected from the cell temperature $T = 724$ K. As can be seen from Fig. 3(c) and 3(d) the Doppler widths determined by fitting data to the AVP and SDAVP formulae for Cd–Ar and Cd–Ne do not vary with the pressure. Similar behaviour was also found for Cd–He, Cd–N_2 and Cd–CH_4. This means that in all these systems the correlation effects do not play any role.

5.2. Broadening and shifting cross sections

The Lorentzian width $\langle\gamma\rangle$ and shift $\langle\Delta\rangle$ of the 326.1 nm Cd line determined by fitting the data to the four theoretical profiles: VP, AVP, SDVP and SDAVP were found to be linearly dependent on the density N of perturbing gas. From the slopes representing these linear dependences the broadening ($\beta = \langle\gamma\rangle/N$) and shift ($\delta = \langle\Delta\rangle/N$) coefficients were determined in Ref. [11–14]. In the present work we used these coefficients to determine the cross sections $\langle\sigma_b\rangle$ and $\langle\sigma_s\rangle$ for the broadening and shifting, respectively. Their values are listed in Table I.

It should be noted that evaluation of experimental profiles by means of the SDAVP requires the assumption of the form of $\Delta V(r)$ the difference of adiabatic potentials. To this end we used van der Waals (vdW) potential with C_6 constants calculated both in the Coulomb Approximation (CA) and with the Hartree–Fock (H–F) wave functions as well as numerical *ab initio* potentials calculated by Czuchaj and Stoll (C–S) [15]. We also used the Morse potential with force constants determined by Koperski *et al.* [16] from their experiments on Cd-rare gas excimers produced in supersonic expansion beams. These potentials were also used to calculate the β and δ coefficients as well as the cross sections $\langle\sigma_b\rangle$ and $\langle\sigma_s\rangle$ on the basis of the impact theory corrected for the collision-duration time effect [25]. Results of such calculations are listed in Table II.

Comparison of Tables I and Table II shows that — although quite a reasonable agreement between theory and experiment was found for some coefficients in the case of Cd–Xe and Cd–Kr systems for vdW and C–S potentials — generally there is poor agreement between experimental and theoretical values both for β and δ coefficients. It is interesting to note a fairly good agreement between experimental values of β and δ for molecular perturbers H_2, D_2, and N_2 with theoretical ones calculated on the basis of the vdW potential.

In order to get more insight into the mechanisms responsible for the observed effects we have analysed the influence of polarizability ξ of the perturbing particle on the broadening and shifting cross sections. To this end we have plotted the cross sections $\langle\sigma_b\rangle$ and $\langle\sigma_s\rangle$ on the quantity $(\xi/\langle v\rangle)^{2/5}$ as

TABLE I

Experimental values of β and δ (in units 10^{-20} cm^{-1}/atom cm^{-3}), κ (units 10^{-21} /atom cm^{-3}), σ_b and σ_s (units 10^{-14} cm^2).

Perturber	Profile	β	δ	κ	σ_b	σ_s
He	AVP	1.155(34)	−0.031(9)	0.62(34)	0.702(21)	0.038(11)
Ne	AVP	0.715(4)	−0.090(5)	0.17(7)	0.710(4)	0.179(10)
Ar	AVP	1.060(6)	−0.387(4)	−0.30(5)	1.388(8)	1.014(11)
Kr	AVP	1.159(11)	−0.329(5)	−1.16(7)	1.939(19)	1.101(17)
	SDAVP--vdW	1.146(10)	−0.341(5)	−0.94(7)	1.917(17)	1.141(17)
	SDAVP--CS	1.147(11)	−0.338(5)	−1.00(7)	1.919(19)	1.131(17)
Xe	AVP	1.273(7)	−0.333(2)	−1.42(8)	2.394(14)	1.252(8)
	SDAVP--vdW	1.258(6)	−0.344(2)	−1.16(7)	2.366(12)	1.294(8)
	SDAVP--CS	1.257(6)	−0.348(2)	−1.08(7)	2.364(12)	1.309(8)
H_2	VP	1.73(8)	−0.06(9)	—	0.74(4)	0.05(8)
D_2	VP	1.34(6)	−0.25(7)	—	0.80(4)	0.30(9)
N_2	AVP	1.054(9)	−0.281(7)	−0.36(8)	1.526(14)	0.814(21)
CH_4	AVP	1.548(5)	−0.446(4)	−0.81(7)	1.770(6)	1.020(10)

shown in Figs. 4 and 5. According to Eqs. (8) and (9) for the van der Waals potential such plots should be represented by straight lines such that the ratio of their slopes is equal to Lorentzian width to shift ratio $\langle\gamma\rangle/\langle\Delta\rangle = 2.7528$. The values of polarizabilities ξ for which the plots were made are listed in Table II. For all perturbing gases except H_2 and D_2 we used experimental values of ξ given in Ref. [29]. For H_2 and D_2 we used theoretical values calculated by Kołos and Wolniewicz [30]. The straight lines marked by "1" in Figs. 4 and 5 represent the theoretical dependence computed from Eqs. (8) and (9) using he C_6 constants calculated in the framework of the Coulomb approximation. The straight lines marked by "2" represent least-squares linear fits of the data.

TABLE II

Theoretical values of β, δ, κ, σ_b, σ_s (units as in Table I). Units of polarizabilities ξ are (10^{-24} cm^3).

Perturber	ξ	β	δ	κ	σ_b	σ_s	Potential
He	0.216	0.664	−0.241	−0.01	0.404	0.293	vdW (CA)
		0.853	−0.310	−0.14	0.518	0.377	vdW (H-F)
		0.726	−0.286	−0.07	0.441	0.348	Morse
		1.094	0.059	0.083	0.665	0.072	C–S
Ne	0.398	0.644	−0.234	−0.20	0.639	0.465	vdW (CA)
		0.828	−0.301	−0.59	0.822	0.598	vdW (H–F)
		0.734	−0.063	0.06	0.729	0.125	Morse
		0.750	−0.142	−0.025	0.745	0.282	C–S
Ar	1.63	0.964	−0.350	−0.55	1.263	0.917	vdW (CA)
		1.239	−0.449	−0.80	1.623	1.176	vdW (H–F)
		1.439	−0.204	−0.70	1.885	0.534	Morse
		1.334	−0.358	−0.85	1.747	0.938	C–S
Kr	2.48	0.976	−0.354	−0.64	1.633	1.184	vdW (CA)
		1.255	−0.454	−1.18	2.100	1.519	vdW (H–F)
		1.838	−0.214	−1.39	3.075	0.716	Morse
		1.182	−0.181	−0.99	1.977	0.606	C–S
Xe	4.01	1.113	−0.403	−1.17	2.093	1.516	vdW (CA)
		1.431	−0.517	−1.70	2.691	1.944	vdW (H–F)
		1.101	−0.221	−0.89	2.070	0.831	Morse
		1.330	−0.322	−1.15	2.501	1.211	C–S
H_2	0.806	1.42	−0.52	—	0.608	0.46	vdW (CA)
D_2	0.796	1.15	−0.42	—	0.690	0.50	vdW (CA)
N_2	1.76	0.933	−0.338	-0.60	1.351	0.979	vdW (CA)
CH_4	2.59	1.255	−0.455	−0.66	1.435	1.041	vdW (CA)

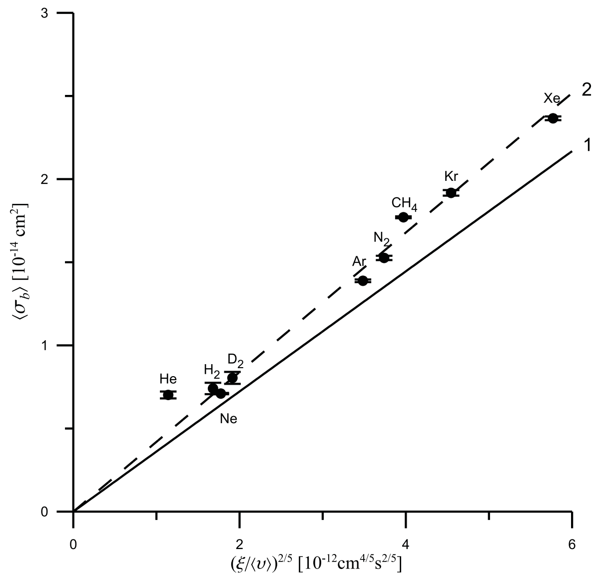

Fig. 4. Broadening cross-section $\langle\sigma_b\rangle$ averaged over Maxwellian distribution of reduced velocities x *versus* $(\xi/\langle v\rangle)^{2/5}$. Straight line (——) — theoretical values, dots (•) — experimental values, dashed line (– – –) — best fit to the experiment.

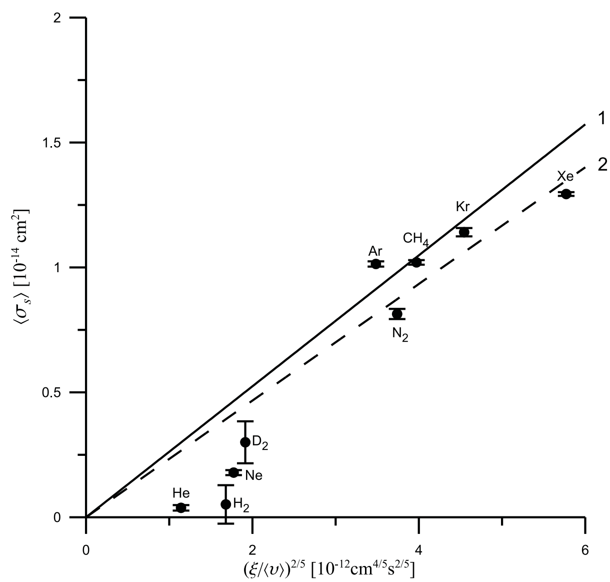

Fig. 5. Shift cross section $\langle\sigma_s\rangle$ averaged over Maxwellian distribution of reduced velocities x *versus* $(\xi/\langle v\rangle)^{2/5}$. Symbols as in Fig. 4.

The plots shown in Figs. 4 and 5 clearly demonstrate a departure of the real interatomic potential from the van der Waals form. The main conclusion which can be drawn from such an analysis is that it is not possible to interpret in a consistent way the shift and broadening data using a van der Waals potential alone, although in some cases the agreement with experiment is fairly good.

5.3. Collision-time asymmetry coefficients

Table I contains also the values of the asymmetry coefficient $\kappa = \langle\chi\rangle/N$ which is defined by Eq. (2) and is a measure of the dispersion-shaped correction to the Lorentzian component of the total line profile. This coefficient contains information on the interatomic potential and collision dynamics over and above the pressure broadening and shifting coefficients. A minus sign of the coefficient κ indicates *red asymmetry*, *i.e.* a higher intensity in the red wing than in the blue. As it is seen, in the case of hydrogen and deuterium used as perturbing gases no collision-time asymmetry was observed.

Table I shows that in the cases of perturbation by heavier rare gases (Ar, Kr, Xe) as well as by N_2 and CH_4 the asymmetry is in the same direction as the shift, *i.e.* in these cases the 326.1 nm Cd line has a more intense red wing. Contrary to that, for He and Ne the shift (red) and asymmetry ($\kappa > 0$) are in opposite directions. It should be noted that in most experiments on pressure effects on spectral lines so far performed in which helium was used in the role of a perturbing gas a blue shift ($\delta > 0$) was observed and this was usually regarded as an evidence of the importance of the repulsive part in the interaction potential. According to the theory [17–21], for pure repulsion potentials the blue shift should be associated with blue asymmetry ($\kappa > 0$) contrary to what we have observed in our experiment for the Cd–He and Cd–Ne systems. Table II contains theoretical values [25] of the κ-coefficients calculated on the basis of the Czuchaj–Stoll and van der Waals potentials. As seen from Table II the calculations based on the Czuchaj–Stoll potentials predict for Cd–He a blue asymmetry although much smaller than that measured one. On the other hand, the same calculations yielded the blue shift while the red ($\delta < 0$) one was observed in experiment. We should note that the red shift and the blue asymmetry of a spectral line shape induced by helium were observed by the Lewis group [7–9] for the 422.7 nm calcium line. More recently, Romalis *et al.* [6] observed the blue asymmetry for the D_1 and D_2 lines of rubidium perturbed by the ^{4}He and ^{3}He isotopes, but in their experiments the D_1 and D_2 lines were shifted towards the blue ($\delta > 0$).

6. Conclusion

Using a LIF technique we have made measurements of the shapes of the 326.1 nm cadmium line perturbed by rare gases and some molecular gases (H_2, D_2, N_2, CH_4). The line shapes were found to be inadequately described by the ordinary (symmetric) Voigt profile. Two distinct sources of line shape asymmetry have been identified and analysed in detail. We have shown that the asymmetric speed-dependent Voigt profile, Eq. (12), provides an excellent description of the 326.1 nm Cd line over a wide range of perturbing gas pressure. We have also shown that the variation of the broadening and shifting cross sections of the same line perturbed by various foreign gases with the quantity $(\xi/\langle v\rangle)^{2/5}$ may serve as an additional source of information on the interatomic interactions. The plots of these two cross sections *versus* $(\xi/\langle v\rangle)^{2/5}$ clearly demonstrate a departure of the real interaction potential from that of the van der Waals form.

This work was supported by the Polish State Committee for Scientific Research (KBN) grant no. 5 P03B 066 20 (354/P03/2001/20).

REFERENCES

[1] J.F. Kielkopf, N.F. Allard, *J. Phys.* **B13**, 709 (1980).

[2] R.E. Walkup, A. Spielfiedel, D.E. Pritchard, *Phys. Rev. Lett.* **45**, 986 (1980); R. Walkup, B. Stewart, D.E. Pritchard, *Phys. Rev.* **A29**, 169 (1984).

[3] T.D. Raymond, N. Böwering, Ch.Y. Kuo, J.W. Keto, *Phys. Rev.* **A29**, 721 (1984).

[4] Y.C. Chan, J.A. Gelbwachs, *J. Phys.* **B25**, 3601 (1992).

[5] A. Schwabedissen, W. Bötticher, *J. Phys.* **B26**, 3467 (1993).

[6] M.V. Romalis, E. Miron, G.D. Cates, *Phys. Rev.* **A56**, 4569 (1997).

[7] M. Harris, E.L. Lewis, D. McHugh, I. Shannon, *J. Phys.* **B17**, L661 (1984); 19, 3207 (1986).

[8] I. Shannon, M. Harris, D.R. McHugh, E.L. Lewis, *J. Phys.* **B19**, 1409 (1986).

[9] E.L. Lewis, *Spectral Line Shapes*, Vol. 5, Ed. J. Szudy, Ossolineum Publishing, Wrocław 1989, p. 485.

[10] J. Boissoles, T. Thibault, C. Boulet, J.P. Bouanich, J.M. Hartmann, *J. Mol. Spectrosc.* **198**, 257 (1999).

[11] A. Bielski, R. Ciuryło, J. Domysławska, D. Lisak, R.S. Trawiński, J. Wolnikowski, *Acta Phys. Pol.* **A97**, 1003 (2000).

[12] R.S. Trawiński, A. Bielski, D. Lisak, *Acta Phys. Pol.* **A99**, 243 (2001).

[13] A. Bielski, D. Lisak, R.S. Trawiński, *Eur. Phys. J.* **D14**, 27 (2001).

[14] A. Bielski, R. Ciuryło, J. Domysławska, D. Lisak, R.S. Trawiński, J. Szudy, *Phys. Rev.* **A62**, 032511 (2001).

[15] E. Czuchaj, H. Stoll, *Chem. Phys.* **248**, 1 (1999).

[16] J. Koperski, M. Czajkowski, *J. Chem. Phys.* **109**, 459 (1998); *Eur. Phys. J.* **D10**, 363 (2000); J. Koperski, Sz.M. Kiełbasa, M. Czajkowski, *Spectrochim. Acta* **A56**, 1613 (2000).

[17] P.W. Anderson, *Phys. Rev.* **86**, 809 (1952); P.W. Anderson, J.D. Talman, *Bell Telephone Systems Report* No. 3117, (1956).

[18] M. Baranger, *Phys. Rev.* **111**, 494 (1958).

[19] J. Szudy, W.E. Baylis, *J. Quant. Spectrosc. Radiat. Transfer* **15**, 641 (1975); **17**, 681 (1977); *Phys. Rep.* **266**, 127 (1996).

[20] A. Royer, *Acta Phys. Pol.* **A54**, 805 (1978).

[21] G. Peach, *J. Phys.* **B17**, 2599 (1984); B.N. Al.-Saqabi, G. Peach, *J. Phys.* **B20**, 1175 (1987).

[22] S.G. Rautian, I.I. Sobelman, *Usp. Fiz. Nauk* **90**, 209 (1966) [*Sov. Phys. Usp.* **9**, 701 (1967)].

[23] P.R. Berman, *J. Quant. Spectrosc. Radiat. Transfer* **12**, 1331 (1972).

[24] J. Ward, J. Cooper, E.W. Smith, *J. Quant. Spectrosc. Radiat. Transfer* **14**, 555 (1974).

[25] R. Ciuryło, J. Szudy, R.S. Trawiński, *J. Quant. Spectrosc. Radiat. Transfer* **57**, 551 (1997).

[26] A. Unsöld, *Physik der Sternatmosphären*, Springer, Berlin 1955.

[27] R. Ciuryło, *Phys. Rev.* **A58**, 1029 (1998).

[28] D.W. Marquardt, *J. Soc. Ind. Appl. Math.* **11**, 431 (1963).

[29] Landolt-Börnstein, *Zahlenwerte und Funktionen, Atom- und Molekularphysik,* Vol. 1, Berlin 1950.

[30] W. Kołos, L. Wolniewicz, *J. Chem. Phys.* **46**, 1426 (1967).

[31] D.G. McCartan, N. Lwin, *J. Phys.* **B10**, L17 (1977).